Title

Cyclin B1/Cdk1 Coordinates Mitochondrial Respiration for Cell-Cycle G2/M Progression

Journal

Developmental Cell, 29(2)

ISSN

1534-5807

Authors

Wang, Zhaoqing
Fan, Ming
Candas, Demet
et al.

Publication Date

2014-04-01

DOI

10.1016/j.devcel.2014.03.012

Peer reviewed

Developmental Cell
Article

Cyclin B1/Cdk1 Coordinates Mitochondrial Respiration for Cell-Cycle G2/M Progression

Zhaoqing Wang,[1,9,10] Ming Fan,[1,9] Demet Candas,[1] Tie-Qiao Zhang,[2] Lili Qin,[1] Angela Eldridge,[4] Sebastian Wachsmann-Hogiu,[2] Kazi M. Ahmed,[3] Brett A. Chromy,[4] Danupon Nantajit,[1] Nadire Duru,[1] Fuchu He,[5] Min Chen,[6] Toren Finkel,[7] Lee S. Weinstein,[6] and Jian Jian Li[1,8,*]

[1]Department of Radiation Oncology, University of California, Davis, Sacramento, CA 95817, USA
[2]Center for Biophotonics Science and Technology, University of California, Davis, Sacramento, CA 95817, USA
[3]Life Sciences Division, Department of Cancer and DNA Damage Response, Lawrence Berkeley National Laboratory, University of California, Berkeley, Berkeley, CA 94720, USA
[4]Department of Pathology and Laboratory Medicine, University of California, Davis, Sacramento, CA 95817, USA
[5]State Key Laboratory of Proteomics, Beijing Proteomics Research Center, Beijing 102206, China
[6]Signal Transduction Section, National Institute of Diabetes and Digestive and Kidney Diseases, National Institutes of Health, Bethesda, MD 20892, USA
[7]Center for Molecular Medicine, National Heart, Lung, and Blood Institute, National Institutes of Health, Bethesda, MD 20892, USA
[8]NCI-Designated Comprehensive Cancer Center, University of California Davis School of Medicine, Sacramento, CA 95817, USA
[9]Co-first authors
[10]Present address: Institute of Biophysics, Chinese Academy of Sciences, Beijing 100101, China
*Correspondence: jijli@ucdavis.edu
http://dx.doi.org/10.1016/j.devcel.2014.03.012

SUMMARY

A substantial amount of mitochondrial energy is required for cell-cycle progression. The mechanisms underlying the coordination of the mitochondrial respiration with cell-cycle progression, especially the G2/M transition, remain to be elucidated. Here, we show that a fraction of cyclin B1/Cdk1 proteins localizes to the matrix of mitochondria and phosphorylates a cluster of mitochondrial proteins, including the complex I (CI) subunits in the respiratory chain. Cyclin B1/Cdk1-mediated CI phosphorylation enhances CI activity, whereas deficiency of such phosphorylation in each of the relevant CI subunits results in impairment of CI function. Mitochondria-targeted cyclin B1/Cdk1 increases mitochondrial respiration with enhanced oxygen consumption and ATP generation, which provides cells with efficient bioenergy for G2/M transition and shortens overall cell-cycle time. Thus, cyclin B1/Cdk1-mediated phosphorylation of mitochondrial substrates allows cells to sense and respond to increased energy demand for G2/M transition and, subsequently, to upregulate mitochondrial respiration for successful cell-cycle progression.

INTRODUCTION

In mammals, cell-cycle progression is dependent on highly ordered events controlled by cyclins and cyclin-dependent kinases (Cdks) (Hartwell and Weinert, 1989). The cyclin B1/Cdk1 complex is shown to specifically regulate the entry into mitosis (Hunt, 1989; Nurse, 1990). Through its cytoplasmic, nuclear, and centrosomal localization, cyclin B1/Cdk1 is able to synchronize different events in mitosis such as nuclear envelope breakdown and centrosome separation (Takizawa and Morgan, 2000). Accumulating evidence suggests that mitochondrial respiration is linked with cell-cycle regulators: cyclin D1 coordinates mitochondrial bioenergetics in G1 progression (Sakamaki et al., 2006), cyclin E controls the formation of high energy-charged mitochondria in the G1/S transition (Mitra et al., 2009), cyclin B1/Cdk1 is involved in the integration of mitochondrial fission with the onset of G2/M transition (Taguchi et al., 2007), and a substantial amount of cyclinB1/Cdk1 remains in the cytoplasm in mitosis and active cyclinB1/Cdk1 kinase is found both in the cytoplasm and nucleus during prophase (Gavet and Pines, 2010). However, whether mitochondrial metabolism cooperates with the process of cell division, especially the mechanism underlying the G2/M phase-regulated mitochondrial bioenergetics, needs to be further investigated.

G1/S and G2/M checkpoints are energy-sensitive and require pronounced bioenergy supply for de novo synthesis of biomasses needed for cell-cycle phase transitions (Sweet and Singh, 1995, 1999). In proliferating mammalian cells, mitochondrial ATP is generated via oxidative phosphorylation (OXPHOS) machinery (electron transportation chain), which is composed of five multisubunit complexes, complex I–complex V (CI–CV). CI is the largest complex, with 46 subunits, and serves as the major entry point of electrons into OXPHOS. A functionally efficient CI in OXPHOS is required not only for overall mitochondrial respiration (Roessler et al., 2010) but also for successful cell-cycle progression (Owusu-Ansah et al., 2008).

In this study, cyclin B1/Cdk1 proteins were found to relocate in the matrix of mitochondria, and an increased influx of mitochondrial cyclin B1/Cdk1 was associated with elevated mitochondrial bioenergetics in G2/M transition. We identified a cluster of CI subunits of OXPHOS as potential cyclin B1/Cdk1 substrates in G2/M-linked mitochondrial activity. Our results suggest that the cyclin B1/Cdk1-mediated phosphorylation of CI subunits is

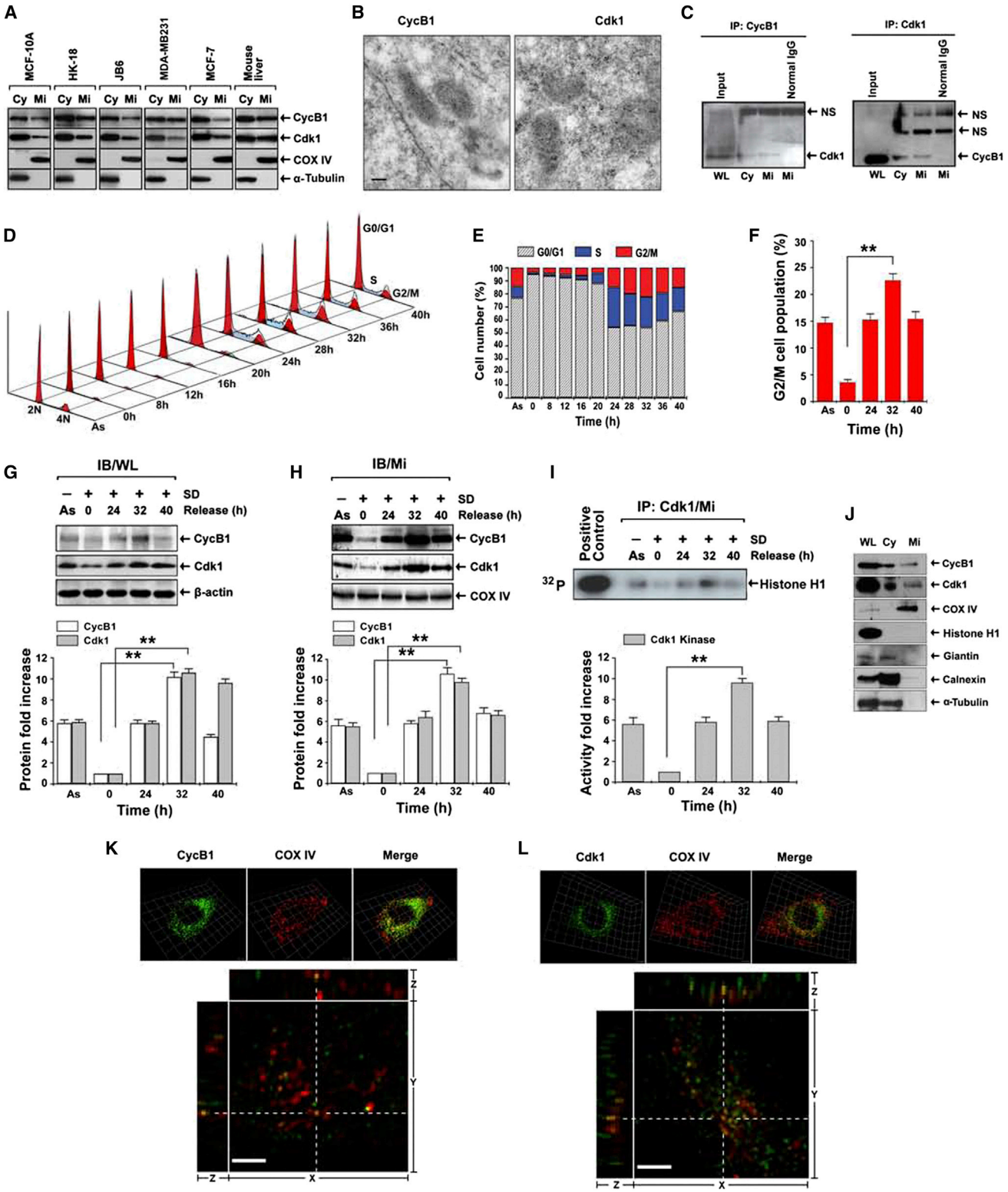

Figure 1. Mitochondrial Cyclin B1/Cdk1 Is Actively Correlated with G2/M Transition

(A) Immunoblotting (IB) analysis of cyclin B1 (CycB1) and Cdk1 of cytosolic (Cy) and mitochondrial (Mi) fractions isolated from an array of human and mouse cell lines and mouse liver tissue (α-tubulin, cytosolic marker; COX IV, mitochondrial marker). MCF-10A cells were used in all further mitochondrial and cell-cycle analyses.

(B) Mi cyclin B1 and Cdk1 detected by immunoelectron microscopy with gold-labeled antibodies (dot arrows, 10 nm gold-particles for cyclin B1 and Cdk1; scale bar represents 250 nm).

(legend continued on next page)

able to upregulate the CI enzymatic activity to enhance mitochondrial energetic homeostasis for G2/M transition. Thus, in addition to their fundamental roles in regulation of cytoplasmic and nuclear events for G2/M transition, cyclin B1/ Cdk1 may also function as a coordinator in orchestrating the mitochondrial bioenergetics for cell-cycle G2/M progression.

RESULTS

Cyclin B1/Cdk1 Is Present in Mitochondria at G2/M Transition

Cyclin B1/Cdk1 protein was detected by immunoblot analysis in the mitochondria from an array of human and mouse cells, including human breast epithelial MCF-10A cells, skin keratinocytes HK18, mouse skin epithelial cells JB6, human breast cancer MDA-MB-231 and MCF-7 cells, as well as in mitochondria isolated from mouse liver tissues (Figure 1A). The mitochondrial localization of cyclin B1 and Cdk1 was confirmed by immunogold labeling electron microscopy (Figure 1B), by double labeling using different sizes of gold particles (Figure S1A available online). Coimmunoprecipitation further showed that cyclin B1 and Cdk1 formed a complex in the mitochondria (Figure 1C), indicating that mitochondrial cyclin B1/Cdk1 should be enzymatically active and able to regulate mitochondrial substrates.

The exquisite control of cyclin B1/Cdk1 activity during the cell cycle to peak at metaphase is necessary for a successful G2/M transition (Allan and Clarke, 2007; Clute and Pines, 1999). To investigate whether changes in mitochondrial abundance of cyclin B1/Cdk1 corresponds with changes in their total cellular protein levels during cell-cycle progression, we synchronized cells at G0/G1 phase by serum deprivation (SD) for 48 hr (Davis et al., 2001) and examined both total cellular and mitochondrial cyclin B1 and Cdk1 levels during different phases of the cell cycle after cells were released from starvation. The results of fluorescence-activated cell sorting (FACS) revealed that the G2/M population peaked at 32 hr after release from G0/G1 synchronization (Figures 1D–1F) and showed the highest levels of cyclin B1 and Cdk1 proteins in mitochondria (Figures 1G and 1H). Consistent with this, mitochondrial Cdk1 kinase activity was maximal at the same time point (Figure 1I).

The purity of the mitochondrial preparations was confirmed using markers from several subcellular components. COX IV, a mitochondrial resident protein, was detected exclusively in the mitochondrial preparation, whereas histone H1, a nuclear protein, was only detected in whole lysate but not in other fractions. Giantin (a Golgi apparatus protein), calnexin (an endoplasmic reticulum protein), and α-tubulin (a cytoskeleton protein) were all absent in the mitochondrial fraction but detected in the cytoplasmic fraction. The results indicate that our preparations yield a relatively high purity of the mitochondria (Figure 1J).

The mitochondrial localization of cyclin B1/Cdk1 was further studied by immunofluorescence assays (IFAs) with double staining using antibodies to cyclin B1 or Cdk1 along with antibodies to COX IV. The results of 3D deconvolution fluorescence microscopy (Figures 1K and 1L, upper panels) showed that cyclin B1 and Cdk1 were colocalized with COX IV in G2/M-enriched cells at 32 hr. Using structured illumination superresolution fluorescence microscopy, we observed that cyclin B1 and Cdk1 localized in the near proximity of COX IV. The average distance between COX IV and cyclin B1 or Cdk1 was calculated to be <350 nm, which is significantly below the lower limit of the size of a mitochondrion (600–1,000 nm) (Kennady et al., 2004). In addition, some merged dots of cyclin B1/Cdk1 and COX IV colocalization were also observed on orthogonal views (xy, yz, and xz planes in Figures 1K and 1L, lower panels; Movies S1 and S2). The images in Figures 1K and 1L are representative z sections showing the colocalization of COXIV and cyclin B1/Cdk1 complex in the mitochondria.

To achieve optimal resolution for observing mitochondrial localization of cyclin B1/Cdk1, we used thin optical sectioning to achieve 30–40 z sections along the Z direction across a whole cell. Cyclin B1 and Cdk1 staining in the nucleus was not visible on the representative z sections in Figures 1K and 1L, but could be seen on the image of the same cell with 0.5 μm up in the z section (Figure S1B). The centrosome-like structures stained by anti-cyclin B1 or anti-Cdk1 antibodies were also visible at different z sections (Figures S1C and S1D). As the z value increased from Z = 0, the centrosome-like structures gradually disappeared (Figures S1C and S1D). The staining of cells at different stages of the cell cycle, late S phase, prometaphase, and metaphase, revealed the known pattern of cyclin B1 localization on the centrosomes, mitotic spindle and DNA (Figure S1E), indicating the specificity of the cyclin B1 antibody used in this study. Collectively, the data obtained from various approaches indicate that a fraction of cyclin B1/Cdk1 proteins is present in the mitochondria, and an increased mitochondrial

(C) Immunoprecipitation (IP) of cyclin B1 followed by IB of Cdk1 or reverse using whole cell lysates (WL), cytosolic (Cy) and mitochondrial (Mi) fractions (NS, nonspecific binding).
(D–F) Cell-cycle distribution after release from G0/G1 synchronization (As, asynchronous cells) with G2/M population peaked at 32 hr (F) (mean ± SD; n = 3; $^{**}p < 0.01$).
(G and H) IB of cyclin B1 and Cdk1 in whole cell lysates (WL, G) and Mi fraction (H) at indicated times after release from G0/G1 synchronization.
(I) Kinase assay of Mi Cdk1 isolated by IP after release from G0/G1 synchronization (Histone H1, control substrate; commercial Cdk1, positive control). The lower panels show estimated fold changes of protein expression (G and H) and Cdk1 kinase activity in autoradiography (I) using Image software (mean ± SD; n = 3; $^{**}p < 0.01$).
(J) Cyclin B1 and Cdk1 in WL, Cy, and Mi fractions isolated from G2/M-peaked cell populations were detected by IB together with markers histone H1 (nuclear protein), COX IV, (Mi marker), giantin (Golgi apparatus membrane marker), calnexin (endoplasmic reticulum membrane marker), and α-tubulin (Cy marker).
(K and L) Mitochondrial localization of cyclin B1 and Cdk1 detected by immunofluorescence using 3D structured illumination superresolution microscopy. Upper panels: fluorescence images of immunostained mitochondrial cyclin B1 (K) and Cdk1 (L) isolated from G2/M-enriched cells with COX IV as control. Lower panels: the raw fluorescence images were also deconvoluted with a proprietary software package to enhance the resolutions. Yellow dots from merged images represent colocalization of cyclin B1/Cdk1 and COX IV from orthogonal views (xy, yz, and xz planes).
See also Figure S1 and Movie S1.

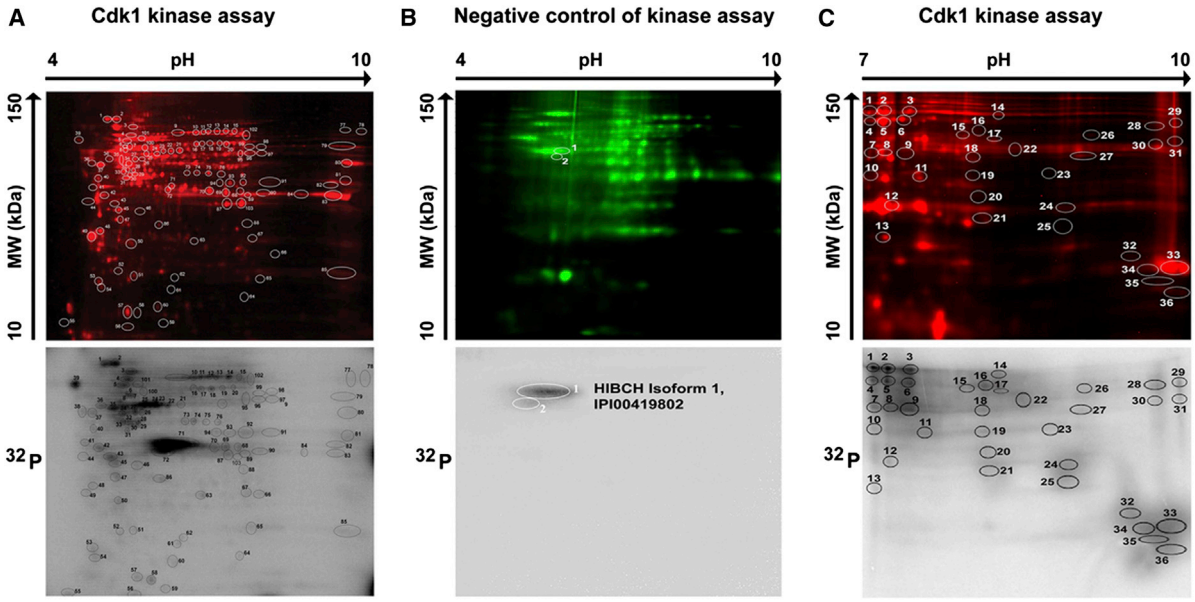

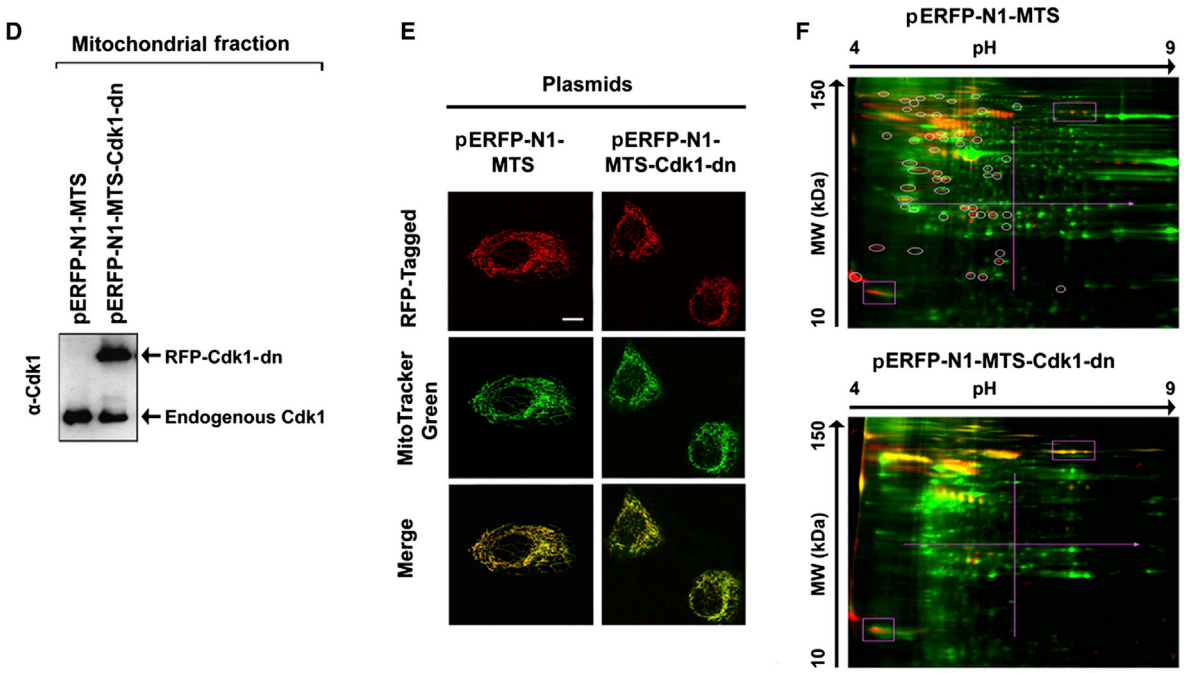

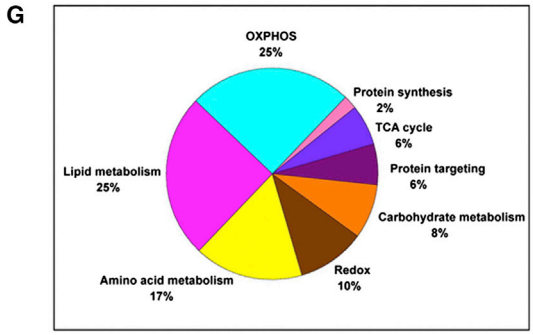

H

OXPHOS machinery	Subunits number	CyclinB1/Cdk1 Substrates
Complex I	46	8
Complex II	4	0
Complex III	11	2
Complex IV	13	0
Complex V	16	2

(legend on next page)

influx of cyclin B1/Cdk1 is associated with the progression of G2/M transition.

Potential Mitochondrial Targets of Cyclin B1/Cdk1

A repertoire of mitochondrial proteins is phosphorylated during mitosis (Dephoure et al., 2008). Cdk1 belongs to the serine/threonine (S/T) kinase family catalyzing the transfer of a phosphate from ATP to proline (P)-oriented S or T residues. Its substrates contain either an optimal (S/T*-P-x-K/R; x, any residue) or a minimal (S/T*-P) Cdk1 consensus motif. To identify potential cyclin B1/Cdk1 targets in mitochondria, we incubated commercially obtained Cdk1 with mitochondrial proteins isolated from G0/G1 cells that possessed low endogenous cyclin B1/Cdk1 activity in vitro. Triplicate Cdk1 kinase assay products were analyzed by 2D gel analysis with pH 4–10 gel strips, which generated about 110 spots with incorporated [γ-^{32}P] ATP (Figure 2A). In a negative control kinase assay, in which Cdk1 activity was blocked by treatment with the Cdk1 inhibitor RO-3306, only two spots (one protein) among the 110 spots identified were phosphorylated by endogenous mitochondrial kinases other than Cdk1 (Figure 2B). Further 2D gel analysis with pH 7–10 gel strips revealed 36 proteins that incorporated [γ-^{32}P] ATP (Figure 2C). Mass spectrometric study showed that Cdk1 potentially phosphorylates 52 different proteins out of the total 146 spots after exclusion of multiple spots that correspond to the same proteins. The results of Scansite search (http://scansite.mit.edu) indicated that all of the 52 Cdk1 substrates contain at least one minimal consensus site and among them 19 substrates (including eight CI subunits) contain an optimal Cdk1 consensus phosphorylation motif (Table S1).

A point mutation that replaces an aspartate (D) residue with asparagine (N) at position 146 of Cdk1 (D146N) generates a dominant negative (dn) Cdk1 mutant (van den Heuvel and Harlow, 1993). To study function of mitochondrial Cdk1, we generated a mitochondria-targeted Cdk1-dn by constructing a plasmid (pERFP-N1-MTS-Cdk1-dn) containing a 29 amino acid-long mitochondrial targeting sequence (MTS) derived from the subunit VIII of the human cytochrome C oxidase linked to RFP-tagged dn-Cdk1. pERFP-N1-MTS with mitochondria-targeted ERFP only was used as an empty vector control (Figures 2D and 2E). Mitochondrial phosphoproteins in G2/M cells transfected with both constructs were profiled by 2D gel analysis. Compared with mock transfectants (Figure 2F, upper panel), a group of mitochondrial phosphoproteins was apparently absent or decreased in the Cdk1-dn transfectants (Figure 2F, lower panel). Mass spectrometry analysis of the spots detected in Figure 2F revealed that 15 of the in vivo cyclin B1/Cdk1-phosphorylated mitochondrial proteins (Table S2) were among the list of proteins detected with the in vitro kinase assay (Table S1). Thus, our results of phosphoproteomics identified a specific cluster of mitochondrial proteins that were potentially phosphorylated by cyclin B1/Cdk1, including elements of OXPHOS (mitochondrial respiration chain), proteins involved in the metabolism of lipids, amino acids, and carbohydrates, the tricarboxylic acid cycle, and redox balance. Among these 52 potential substrates (Figure 2G), 12 targets belonged to the OXPHOS machinery including the five major respiratory complexes (CI, CII, CIII, CIV, and CV) (Figure 2H). Intriguingly, eight of the identified OXPHOS targets were CI subunits and they all contained the optimal Cdk1 consensus phosphorylation motif (Table S3) determined by Scansite search, suggesting that cyclin B1/Cdk1 regulates mitochondrial ATP generation via activation of CI.

Cyclin B1/Cdk1 Localizes in the Mitochondrial Matrix and Phosphorylates CI Subunits in the Mitochondrial Respiration Chain

Consistent with the increased mitochondrial influx of cyclin B1/Cdk1 proteins and Cdk1 kinase activity at G2/M phase (Figures 1G–1I), the overall mitochondrial phosphoprotein levels were markedly enhanced in G2/M-enriched cells (32 hr) compared to the G0/G1 cells (0 hr) (Figure 3A). To determine the submitochondrial localization of cyclin B1/Cdk1, we prepared the submitochondrial fractions using the alkaline extraction method with the soluble proteins recovered in the supernatant. Timm13 subunit of the translocase of inner membrane (TIM) complex, which resides in the inner membrane space; and Tom40 subunit of the translocase of outer membrane (TOM) complex, residing on the outer membrane, were used as markers of submitochondrial compartments. Unlike Tom40 in the pellets, the presence of cyclin B1/Cdk1 in the supernatant excluded the possibility of its outer membrane localization (Figure 3B) and suggest cyclin B1/Cdk1 to be either soluble proteins that localize in the matrix like Hsp60, or integral membrane proteins that reside in the inner

Figure 2. Potential Mitochondrial Substrates of Cdk1

(A) Mitochondrial (Mi) proteins (1 mg) isolated from G0-G1 cells were incubated with commercial Cdk1 in the presence of [γ-^{32}P] ATP, of which 50 μg was separated by 2D gel electrophoresis (pH 4–9) after being labeled with Cy5 (upper panel). The phosphorylated spots were detected by autoradiography (lower panel) and the circled spots were extracted and further analyzed by mass spectrometry and a cluster of potential Cdk1-phosphorylated mitochondrial proteins is listed in Table S1.

(B) A negative control of (A) with the absence of commercial Cdk1 and presence of the Cdk1 inhibitor RO-3306.

(C) Cdk1-Mi target proteins detected with the same Cdk1 kinase assay as (A) with electrophoresis in the range pH 7–10.

(D) Immunoblotting analysis of Cdk1 in Mi fractions isolated from cells transfected with mitochondria-targeted (MTS) dominant negative mutant Cdk1 and empty vectors.

(E) Representative images of cells transfected with the empty vector pERFP-N1-MTS or pERFP-N1-MTS-Cdk1-dn used in (D).

(F) Mi proteins extracted from G2/M-peaked cells transfected with mitochondria-targeted empty vector (pERFP-N1-MTS, upper panel) or mutant Cdk1 (pERFP-N1-MTS-Cdk-dn, lower panel) were labeled with Cy5 (green), separated by 2D gel and phosphorylated proteins were stained with Pro-Q Diamond dye (red). Spots absent in the Mi profile of cells with mitochondria-targeted mutant Cdk1 compared with the vector control transfectants (circled) were extracted and analyzed by mass spectrometry. The potential Cdk1 mitochondrial targets detected by these experiments were listed in Table S2.

(G) Summary of potential Cdk1-targeted mitochondrial proteins detected by in vitro (A–C) and in vivo (E and F) Cdk1 kinase assays.

(H) Distribution of potential mitochondrial Cdk1 targets in the subunits of OXPHOS complexes.

See also Tables S1–S4.

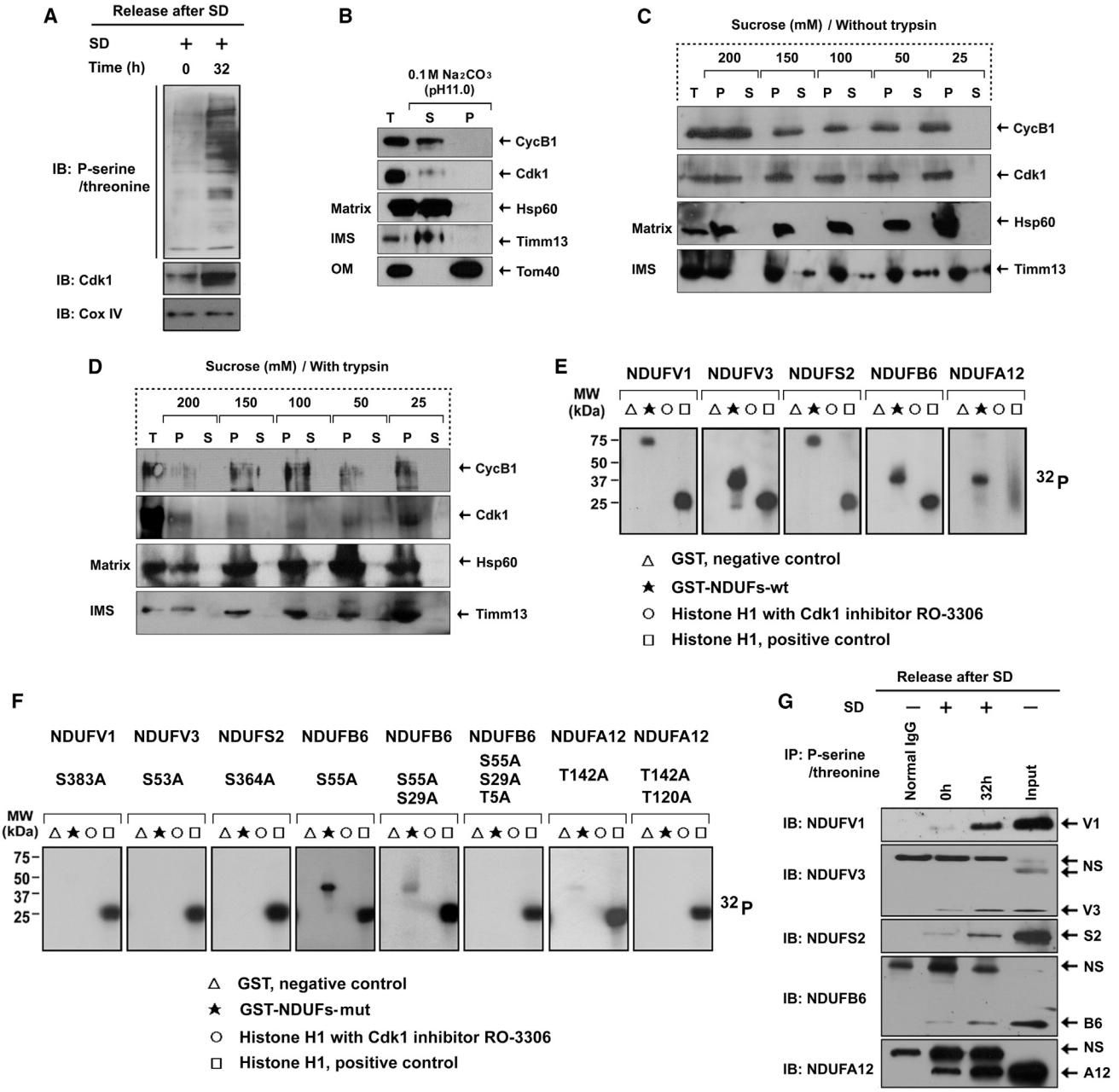

Figure 3. Mitochondrial Cyclin B1/Cdk1 Localizes in the Matrix and Phosphorylates CI Subunits at G2/M Transition

(A) Immunoblotting of mitochondrial (Mi) phosphoserine/threonine proteins isolated from G0/G1 (0 hr) and G2/M (32 hr) cells after release from G0/G1 synchronization.

(B) Submitochondrial localization of cyclin B1 and Cdk1 detected by alkaline extraction (Antonyuk et al., 2013). Matrix proteins were separated from integral membrane proteins by extracting mitochondria with sodium carbonate (pH 11), then the total input (T), soluble matrix proteins (S), and membrane vesicle pellets (P) were immunoblotted for cyclin B1, Cdk1, Tom40 (an outer membrane protein), TIMM13 (an interspace protein), and HSP60 (a matrix protein).

(C and D) Submitochondrial localization of cyclin B1 and Cdk1 detected by mitoplasting and protease protection assay. Mitochondria were incubated in gradient hypotonic sucrose buffer as indicated to digest the outer membrane of mitochondria with or without soybean trypsin. The total (T), pellet (P), and supernatant (S) fractions were subjected to IB analysis with indicated antibodies.

(E and F) Five GST-fused human wild-type CI subunits (E) and their mutants (F) in the indicated potential Cdk1 phosphorylation sites (note, multiple mutations created in NDUFB6 and NDUFA12) were synthetized and tested as substrates in kinase assay with commercial Cdk1.

(G) Mitochondrial proteins from G0/G1 and G2/M cells were extracted by IP using a phosphoserine/threonine antibody followed by IB using antibodies to each of the five CI subunits (normal IgG, control for the IP reaction; NS, nonspecific band).

See also Figure S2 and Table S3.

membrane like Timm13 (Figure 3B). To further specify the submitochondrial localization of cyclin B1 or Cdk1, we performed mitoplasting by diluting mitochondria in hypotonic buffers with decreasing concentrations of the osmoticum sucrose from 200 mM to 25 mM. The outer membrane began to rupture at 150 mM of sucrose, while the inner membrane remained intact until the final concentration at 25 mM of sucrose (Figure 3C). In combination with mitoplasting, protease protection assay was performed using trypsin to digest exposed proteins following outer membrane rupture. Similar with Hsp60 but unlike Timm13, cyclin B1 and Cdk1 were protected from trypsin digestion, indicating their mitochondrial matrix localization (Figure 3D).

To validate the phosphorylation of aforementioned eight CI subunits by Cyclin B1/Cdk1 complex, we constructed these CI subunits as GST fusion proteins and expressed them in *Escherichia coli* (Figure S2). Among them, five of the synthesized CI subunits were expressed as soluble proteins and can be phosphorylated by in vitro Cdk1 kinase assay (Figure 3E). These results were confirmed by generating phosphorylation defective forms of the five CI subunits through substitutions of S/T residues with Alanine (A) on either Cdk1 optimal or minimal consensus motifs (T383 on NDUFV1, S105 on NDUFV3, S364 on NDUFS2, S55/S29/T5 on NDUFB6, and T142/T120 on NDUFA12). The mutation of Cdk1 consensus motifs severely diminished their phosphorylation (Figure 3F). Consistent with the increased influx and activity of Cyclin B1/Cdk1 in mitochondria, the phosphorylation levels of the five endogenous CI subunits were increased in G2/M transition compared to G0/G1 phase (Figure 3G). Collectively, these data demonstrate that during G2/M transition, an increased influx of Cyclin B1/Cdk1 into the mitochondrial matrix promotes phosphorylation of CI subunits, which may facilitate electron transport through the mitochondrial respiration chain.

Cyclin B1/Cdk1-Mediated CI Phosphorylation Is Required for CI Function

CI is the major entry point of electrons into the respiratory chain and plays a fundamental role in mitochondrial ATP generation (Janssen et al., 2006). To investigate cyclin B1/Cdk1-mediated regulation of CI activity, we constructed plasmids expressing GFP-tagged CI subunits, each with three different forms, i.e., wild-type (WT), phosphorylation-mimetic D form (S/T to D), and phosphorylation-defective A form (S/T to A). The mitochondrial localization of each GFP-tagged CI subunit was confirmed by confocal microscopy (Figure 4A), and the transfection efficiency was analyzed by immunoblotting (Figure 4B). As expected, in vivo phosphorylation of each subunit at G2/M phase was inhibited in cells transfected with Cdk1 small interfering RNA (siRNA) (Figure 4C, lane 3), which arrested cells at the G2/M phase (Figure S2). The phosphorylation defective mutant subunits showed no phosphorylation in both G0/G1 and G2/M phases (Figure 4C, lanes 4–5). To address whether phosphorylation of CI subunits is required for CI activity, we tested the ability of WT and phosphorylation-defective CI subunits to rescue CI activity in cells in which the five respective endogenous CI subunits were knocked down by siRNAs targeting their 5′ or 3′ UTRs (Figure 4D). siRNA treatments resulted in 65%–82% reduction in CI activity when compared to cells transfected with the scrambled siRNA-treated empty vector pEGFP-N1-MTS (Figure 4E). Reconstituting each of the CI subunits with their respective WT or D forms significantly rescued the diminished CI activities, while the phosphorylation-defective A form mutants failed to restore CI activities, indicating that CI activity is dependent on Cdk1-mediated phosphorylation of the CI subunits.

Cyclin B1/Cdk1 Coordinates CI Activity with G2/M Transition

To determine whether mitochondrial cyclin B1/Cdk1 is sufficient to induce CI activity at G2/M transition, we examined the correlation between mitochondrial cyclin B1/Cdk1 abundance and CI activity in vitro. To mimic the peak levels of mitochondrial cyclin B1/Cdk1 at G2/M transition, we transfected cells with MTS-oriented cyclin B1/GFP and/or Cdk1/RFP constructs. Targeting of cyclin B1/GFP and Cdk1/RFP to mitochondria was confirmed by immunoblotting (Figure 5A) and confocal microscopy (Figure 5B). As shown in Figure 5C, compared with the empty vector transfectants (lanes 1, 3, and 6), CI activity was enhanced by 174%, 169%, and 242% in cells expressing mitochondrial cyclin B1 alone (lane 2), Cdk1 alone (lane 4), and cyclin B1/Cdk1 (lane 7), respectively. In contrast, mitochondrial mutant Cdk1-dn alone or in combination with cyclin B1 did not affect CI activity (lanes 5 and 8), suggesting a positive coordination between mitochondrial cyclin B1/Cdk1 activity and CI activity.

Consistent with the timing of maximal mitochondrial cyclin B1/Cdk1 at 32 hr after synchronization (Figures 1H–1J), CI activity was at its peak value in G2/M (32 h) cells that were left untreated or mock-transfected with empty vector (pERFP-N1-MTS). To further confirm that the increase of CI activity at G2/M transition was mitochondrial cyclin B1/Cdk1-dependent, we showed that G2/M-related enhancement of CI activity was completely absent in synchronous cells expressing mitochondrial mutant Cdk1-dn (Figure 5D).

Cyclin B1/Cdk1 Enhances Mitochondrial Respiration for G2/M Transition

ATP is generated by OXPHOS through coupling of electron transport with proton (H^+) pumping in the respiration chain, which creates mitochondrial membrane potential ($\Delta\Psi m$) and increases oxygen consumption and reactive oxygen species (ROS) formation. To investigate whether cyclin B1/Cdk1-mediated phosphorylation is required for increased mitochondrial respiration during G2/M transition, we tested the mitochondrial functions in cells transfected with MTS-cyclin B1, MTS-Cdk1-wt, and/or MTS-Cdk1-dn, alone or in combination with each other. Similar to altered CI activity (Figures 5C and 5D), mitochondrial oxygen consumption, $\Delta\Psi m$, and ATP generation were reduced by treatment of cells with Cdk1 inhibitor RO-3306 (Figures 6A–6C), confirming that Cdk1 activity is required for normal mitochondrial respiration. In contrast, mitochondrial metabolism was markedly increased in accordance with mitochondrial abundance of cyclin B1/Cdk1 due to mitochondria-targeted cyclin B1 (Figures 6D–6F, lane 2), Cdk1 (lane 4), as well as cyclin B1 plus Cdk1 (lane 7), compared with the relative empty vector-transfected control cells (lanes, 1, 3, 6, respectively). Interestingly, a substantial increase in mitochondrial superoxide ($O_2\bullet^-$) levels was only observed in cells cotransfected with MTS-cyclin B1 and MTS-Cdk1 (Figure 6G, lane 7). On the other hand, overexpression of mutant MTS-Cdk1-dn suppressed all of the

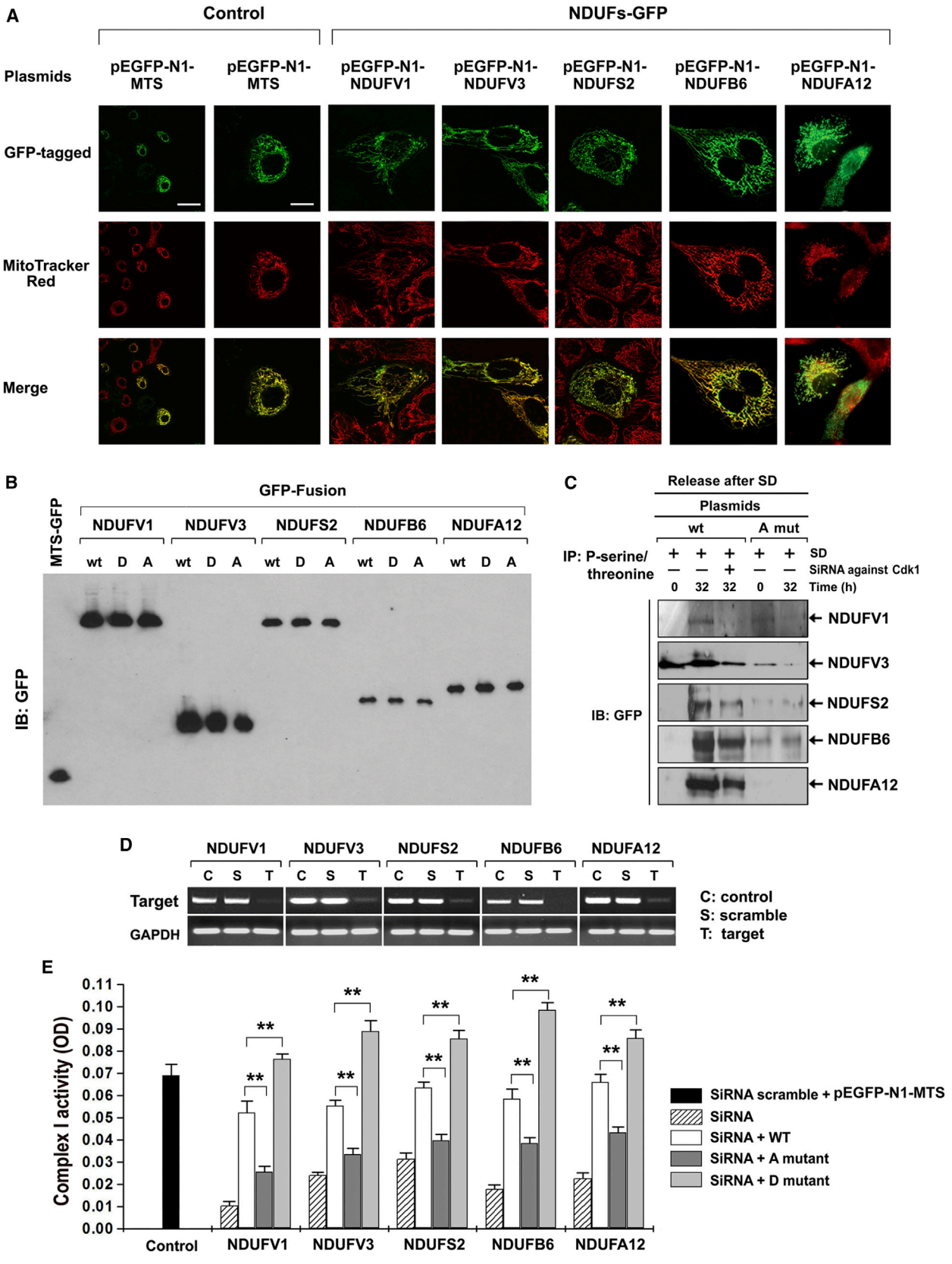

(legend on next page)

tested mitochondrial functions (Figures 6D–6G, lane 5) when compared to control cells (lane 3). Cdk1-dn-mediated mitochondrial suppression could be rescued to levels of mock control cells by cotransfection of cyclin B1 (Figures 6D–6G, lane 8) indicating that cyclin B1 is able to remedy the inhibitory effect of Cdk1-dn (van den Heuvel and Harlow, 1993).

Mitochondrial activity was also tested in synchronized cells transfected with empty vector or MTS-Cdk1-dn vector to study the regulation of mitochondrial activity in conjunction with G2/M transition. Consistent with the positive correlation observed between cyclin B1/Cdk1 abundance and mitochondrial respiration (Figures 6H–6K), endogenous mitochondrial activity was increased in the G2/M-enriched population (32 hr) of cells transfected with empty vector (Figures 6H–6K, S4, and S5). The oxygen consumption rate and ATP generation were more than doubled (Figures 6H and 6I), while the $\Delta\Psi m$ and the superoxide levels were also significantly increased (Figures 6J and 6K). However, this boost of G2/M-associated mitochondrial activities was absent in cells expressing the mitochondria-targeted inactive Cdk1 (Cdk1-dn). Collectively, cyclin B1/Cdk1-mediated enhancement of mitochondrial activity and ATP generation is a predominant feature during G2/M progression of the cell cycle.

Mitochondrial Cyclin B1/Cdk1 Facilitates G2/M Progression

Previous studies have shown that mitochondrial bioenergetics has key roles in cell-cycle progression, mainly in the progression of G1 phase (Schieke et al., 2008; Schulz et al., 2006) and in S phase (Mitra et al., 2009). A recent study showed that mitochondrial oxidative phosphorylation is activated during S and G2/M phases in tumor cells (Bao et al., 2013). To investigate the role of mitochondrial cyclin B1/Cdk1 in mitochondrial metabolism during G2/M progression, we examined cell population kinetics in MCF-10A cells that were transfected with MTS-linked cyclin B1 and/or wild-type or dominant-negative Cdk1 (Figure 7). The results of the cell population study showed that cells constitutively overexpressing mitochondrial WT cyclin B1/Cdk1 had decreased numbers of cells in G1 and increased numbers of cells in S and G2/M phases compared to vector control or mutant cyclin B1/Cdk1 expressing cells (Figures 7A–7D). This expected change in cell-cycle distribution is consistent with accelerated transit through G1 phase, given that G1 phase of the cell cycle is the most responsive phase to changes in cellular metabolic events. We then measured the potential doubling time (Tc) and the duration of each cell-cycle phase, and found that the duration of G1 was on average ~5 hr shorter in cells transfected with WT mitochondrial cyclin B1/Cdk1. Notably, the duration of the S and G2/M phases were also shortened by ~2 hr (Figures 7E and 7F; Table S4) even though these changes in duration did not reflect on the population distribution (Figures 7B and 7C). Although shortened, the S and G2/M phases showed an increased population of cells owing to the more prominent alterations in G1 phase.

To further investigate whether cells progress through G2/M phase faster when mitochondrial cyclin B1/Cdk1 levels are increased, we performed a pulse-chase labeling experiment using a thymidine analog, ethynyl deoxyuridine (EdU), to label the population of cells undergoing DNA synthesis (Terry and White, 2006). This method allows us to visualize a cell cycle captured over a 22 hr window by tracking the EdU-positive population when cells progress through S and G2/M phases and accumulate in G1 phase. The results revealed that labeled S phase cells progressed through G2/M phase and appeared in G1 phase as fast as 4 hr in cells expressing WT mitochondrial cyclin B1/Cdk1, as compared to 6 hr in cells transfected with a vector control or mutant cyclin B1/Cdk1 (Figure 7G), indicating that enhancement of mitochondrial cyclin B1/Cdk1 accelerates G2/M progression. The results of DNA content and EdU labeling analyses suggest that mitochondrial energy supply is a rate-limiting event for cell-cycle progression. Taken together, these results demonstrate that cyclin B1/Cdk1-mediated upregulation of mitochondrial bioenergetics is required for successful cell-cycle progression through G2/M transition.

DISCUSSION

The synchronization of cytoplasmic and nuclear events by temporally and spatially regulated activity of cyclin B1/Cdk1 during G2/M progression has been thoroughly elucidated over decades (Barnes et al., 2001; Baumann, 2012; Draetta and Beach, 1988; Lenormand et al., 1999). Accumulating evidence indicates that not only mitochondrial morphology but also respiration is altered during cell-cycle progression (Garedew et al., 2012; Owusu-Ansah et al., 2008). Notably, ATP production in G2/M phase of colon cancer cells is predominantly dependent on mitochondrial respiration and mitochondrial oxidative phosphorylation is most active during this period, while during G1 phase cells rely more on glycolysis for their energy needs (Bao et al., 2013). The present study defines a mechanism by which cyclin B1/Cdk1 improves mitochondrial respiration and ATP generation to cope with the increased energy demand for

Figure 4. Cdk1-Mediated Phosphorylation of CI Subunits Is Required for CI Activity

(A) Representative images of mitochondria (Mi)-localized CI subunits of transfected cells costained with GFP and Mito Tracker Red (control, empty MTS-GFP vector, scale bar represents 30 μm [left] and 10 μm [right]).

(B) Expression of wild-type or mutant forms of each CI subunit in transfected cells tested by IB of GFP (MTS-GFP, empty vector; WT, wild-type; D, aspartate mutation, constitutive phosphorylation-mimic form; A alanine mutation, phosphorylation-defective form).

(C) Phosphorylated proteins were extracted by IP with phosphoserine/threonine antibody from cells transfected with WT, A, or D mutant CI subunits at 0 hr and 32 hr after release from synchronization, followed by IB for GFP. Cells transfected with wild-type CI and treated with Cdk1 siRNA were included as controls.

(D) RT-PCR analysis of siRNA-mediated inhibition on each of CI subunits.

(E) CI activity rescued by wild-type but not mutant CI subunits. CI activity was measured in cells cotransfected with wild-type or mutant CI subunits along with siRNAs against each of the endogenous CI subunits (see Supplemental Information for a list of CI subunit siRNA sequences). SiRNA scramble + MTS-EGFP, a nontarget control; A mutant, phosphorylation-defective form; D mutant, constitutive phosphorylation-mimic form; one unit of OD is equal to 29.3 μmol/min/mg of proteins (mean ± SD, n = 3; $^{**}p < 0.01$).

See also Figure S3 and Primers of CI in the Supplemental Information.

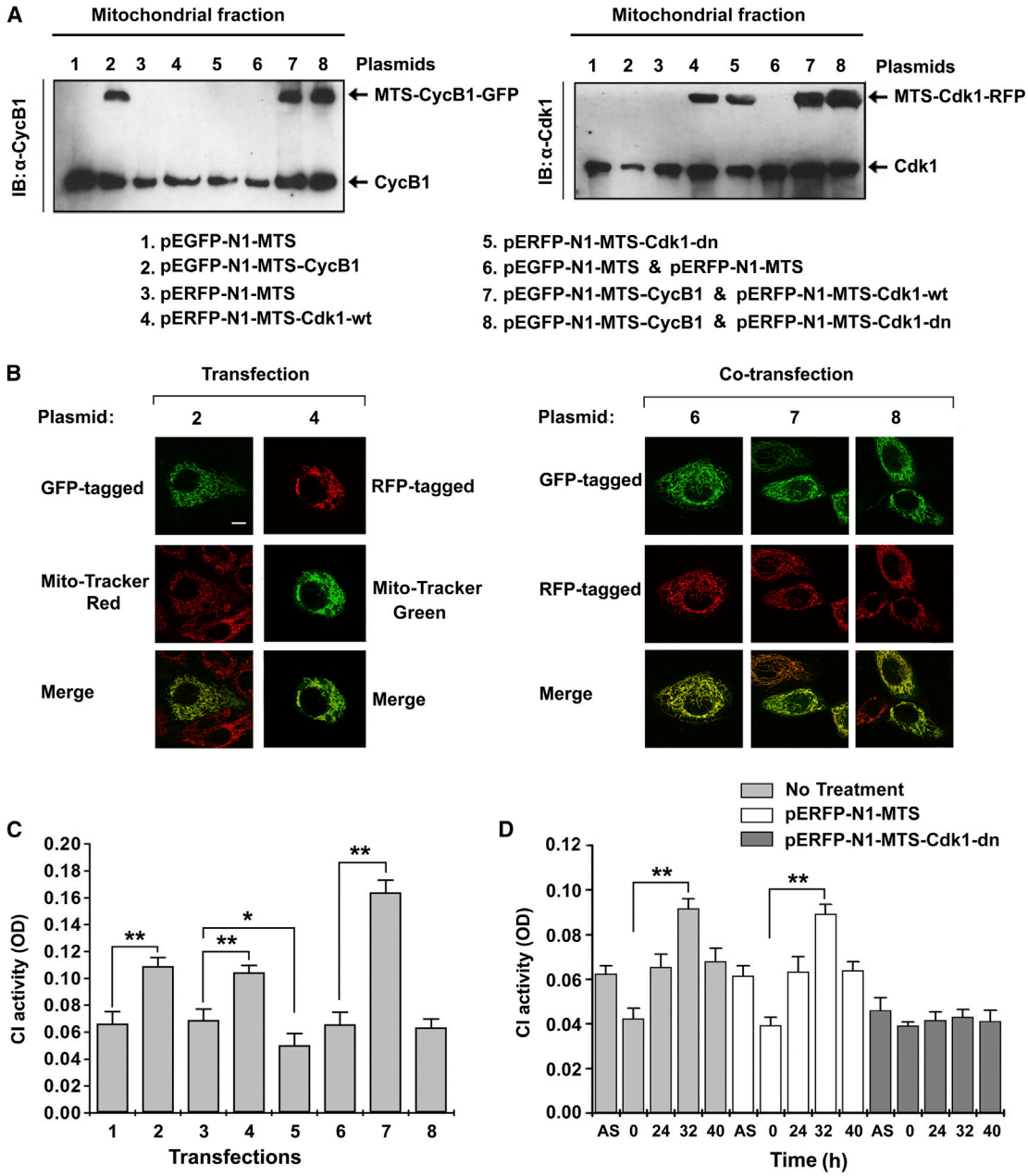

Figure 5. Mitochondrial Cdk1 Is Required for G2/M-Associated CI Activation

(A) IB of mitochondrial fraction isolated from cells for mitochondria-targeted cyclin B1 with wild-type or dominant negative mutant Cdk1 (plasmids are indicated on the bottom. pEGFP-N1-MTS and the pERFP-N1-MTS vectors were empty vector controls for MTS-cyclin B1 and MTS-Cdk1 respectively; see also Supplemental Experimental Procedures for detailed information on the plasmid constructs).

(B) Representative images of mitochondria-localized cyclin B1 (lane 2), Cdk1 (lane 4), or colocalized wild-type and mutant Cdk1 with cyclin B1 (lanes 6–8).

(C) CI activity measured with asynchronous cells 48 hr following transfection of above indicated plasmids (mean ± SD; n = 3; *p < 0.05; **p < 0.01).

(D) CI activity measured in control (no treatment) and in cells with empty vector (pERFP-N1-MTS) or Cdk1-dn mutant (pERFP-N1-MTS-Cdk1-dn) at indicated times after release from G0/G1 synchronization (mean ± SD; n = 3, **p < 0.01).

G2/M transition. We found that both mitochondrial abundance and kinase activity of cyclin B1/Cdk1 was dramatically increased during the G2/M transition. We showed by different approaches that through phosphorylation and activation of five CI subunits involved in OXPHOS, cyclin B1/Cdk1 is able to enhance CI activity and mitochondrial ATP output to meet the increased bioenergy demands required processes during cell division, such as spindle formation and centrosome separation (Nakada et al., 2010).

The subcellular redistribution of cell-cycle regulators is known to be required for checkpoint regulation during cell cycle (Gavet and Pines, 2010). Although cyclin B1 and Cdk1 are expressed

during the late S and G2 phases of the mammalian cell cycle, they become activated during the late G2 phase (Hartwell and Weinert, 1989). The activation of cyclin B1/Cdk1 complex immediately triggers its rapid accumulation into the nucleus via a 40-fold increased rate of nuclear import, a process that is also dependent on Cdk1 activity (Gavet and Pines, 2010). Our results showing redistribution of cyclin B1/Cdk1 to the mitochondrial matrix during G2/M progression provides a mechanism by which critical mitotic events occurring in other cellular compartments can be temporally coordinated with increased mitochondrial bioenergy production during G2/M progression. The timing of mitochondrial influx of cyclin B1/Cdk1 and maximal mitochondrial Cdk1 kinase activity during G2/M transitions (Figure 1) indicates that mitochondrial respiration is coordinated with other cellular processes during this critical phase of cell division.

Cells overexpressing mitochondrial cyclin B1/Cdk1 had a faster G2/M progression than control cells. However, overexpressing dn-Cdk1 in mitochondria resulted in just a slight difference in cell-cycle progression (Figures 7E and 7F), which was unexpected given that mitochondrial protein phosphorylation and respiratory functions were all significantly reduced in cells transfected with dn-Cdk1 (Figures 2F, 5D, and 6H–6K). These apparently discrepant results may well be due to the fact that mitochondrial function and cell-cycle analysis were analyzed in different types of cell populations (synchronous versus asynchronous cell populations, respectively). Using synchronous cells allowed mitochondrial functions to be examined in an enriched G2/M cell population in which a reduction in mitochondrial function in dn-Cdk1 expressing cells could be detected. However, while it was hard to see an inhibitory effect of dn-Cdk1 on cell-cycle progression in asynchronous cells, this may have been more easily observed if we examined this in synchronized cells. Further studies using more suitable cell models are needed to elucidate additional insights underlying the cooperative mechanism between mitochondrial metabolism and progression of different cell-cycle phases via cyclin B1/Cdk1 or other cell-cycle regulators.

Reversible protein phosphorylation plays a key role in the regulation of various mitochondrial functions (Pagliarini and Dixon, 2006). A number of Cdk-phosphorylated proteins have been detected in mitotic HeLa cells (Dephoure et al., 2008). Among them, Drp-1, together with other mitochondrial proteins, is identified to be a target of Cdk1-mediated phosphorylation during early mitosis (Taguchi et al., 2007). In addition, CI subunit NDUFV3 is also identified as a Cdk1 substrate during HeLa cell mitosis (Dephoure et al., 2008), indicating that cyclin B1/Cdk1 targets a multitude of mitochondrial proteins during cell division. However, the functions of the mitochondrial phosphoproteins, especially those involved in cell-cycle-related mitochondrial bioenergetics, remain unknown. In the present study, we identified a cluster of cyclin B1/Cdk1 mitochondrial targets, including those involved in electron transport (CI-CV), tricarboxylic acid cycle, amino acid, and lipid metabolism (Figures 2G and 2H; Table S1). CI functions as the major entry point for electrons into the respiratory chain, and it is also the largest complex in the OXPHOS system. CI dysfunction impairs electron transport, leading to major defects in overall energy metabolism (Janssen et al., 2006). The optimal cyclin B1/Cdk1 phosphorylation motifs are found to be present in the CI subunits; indeed, our data showed that cyclin B1/Cdk1-mediated CI phosphorylation enhanced CI activity. In addition, the mitochondrial matrix localization of cyclin B1/Cdk1 evidently brings it in proximity to the CI that resides on the inner membrane, ensuring the availability of cyclin B1/Cdk1 for a quick response to enhanced cellular ATP demands via phosphorylation of its mitochondrial targets. Therefore, Cdk1-mediated increase in the mitochondrial ATP output is likely a result of upregulated phosphorylation of CI subunits and subsequently enhanced CI activity.

Identification of mitochondrial cyclin B1/Cdk1 substrates is critical for further revealing the mechanistic insights of cell division. In this study, our proteomics approach identified a group of potential Cdk1 mitochondrial targets in G2/M cells, but failed to confirm some of the previously identified known mitochondrial cyclin B1/Cdk1 substrates including Drp-1 (Taguchi et al., 2007), Bad (Konishi et al., 2002), Bcl-2 (Furukawa et al., 2000), Mcl-1 (Harley et al., 2010), and Bcl-xl (Schmitt et al., 2007). This may be potentially due to differences in cell type, context, and the stimulus-dependent nature of interaction of Cdk1 with these substrates. Cdk1 interacts with Bcl-2 in M phase arrested cells (Pathan et al., 2001), with BAD in apoptotic neurons (Konishi et al., 2002) and with Mcl-1 during mitotic arrest (Harley et al., 2010), but none of these interactions have been found in G2/M phase cells. In addition, although Bcl-xl localizes in the outer membrane of mitochondria, its interaction with Cdk1 was shown to occur in the nucleus (Schmitt et al., 2007). It was also shown that cyclin B1/Cdk1 phosphorylates mitochondrial p53 in colon cancer (Nantajit et al., 2010) and survivin in yeast (O'Connor et al., 2002), but we did not detect these to be substrates of mitochondrial cyclin B1/Cdk1 in G2/M phase in MCF-10A cells. A recent study indicates that MnSOD (SOD2), the mitochondrial superoxide dismutase in mammalian cells, can be phosphorylated and activated by cyclin B1/Cdk1 in mitochondria in MCF-10A cells (Candas et al., 2013), and we also identified MnSOD as a cyclin B1/Cdk1 target (Table S1). Along with Cdk1-mediated OXPHOS activation, Cdk1-mediated MnSOD enzymatic activation may be necessary to detoxify the increased superoxide levels generated from enhanced oxidative phosphorylation. Thus, a cyclin B1/Cdk1-regulated OXPHOS-antioxidant network may play an important role in mitochondrial homeostasis and bioenergetics to meet an "extra" cellular fuel demand for cell-cycle progression.

The mechanisms underlying the cyclin B1/Cdk1 mitochondrial influx are largely unknown. Two types of mitochondrial targeting signals (MTSs) have been described: presequences and internal signals (Neupert and Herrmann, 2007; Truscott et al., 2003). Presequences direct precursor proteins into the mitochondrial matrix, inner membrane, or IMS via the TOM complex on the outer membrane. The internal signals, best characterized for members of the carrier family of the mitochondrial inner membrane, are hidden in the mature protein among other amino acid residues important for folding and function. The internal signals can spread throughout the length of the protein. Proteins with MTSs are transferred into mitochondria via interactions with chaperone proteins that can be recognized by the TOM complex (Neupert and Herrmann, 2007; Truscott et al., 2003). Prediction of the mitochondrial localization of cellular proteins can be performed based on the presence of an N-terminal presequence

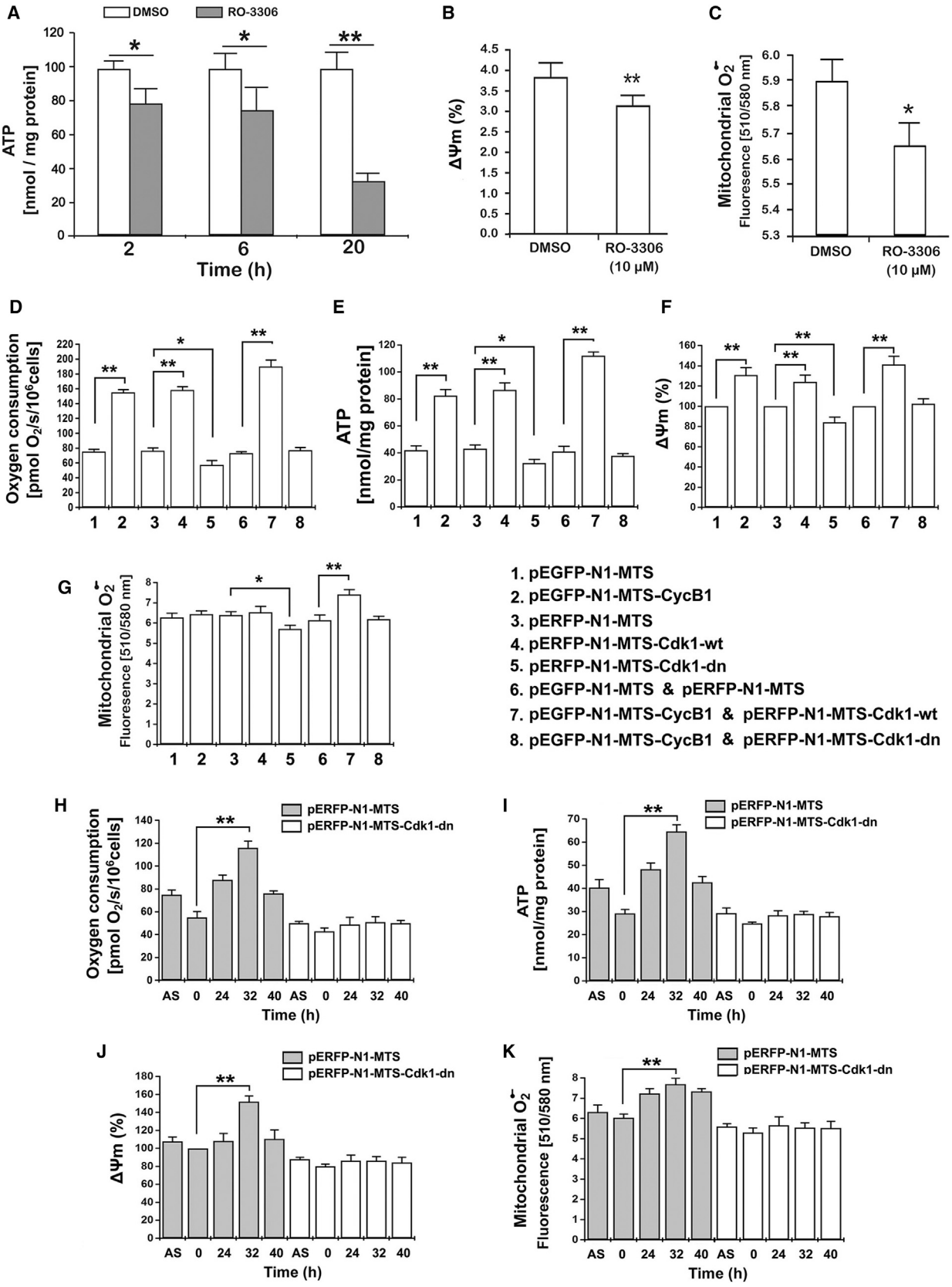

(legend on next page)

(Claros and Vincens, 1996). In this study, we utilized Mitoprot database to search for presequences within cyclin B1 and Cdk1 and found no presequences in Cdk1. However, an N-terminal 42-residue region of cyclin B1 known to be responsible for its cytoplasmic localization and nuclear shuttling (Pines and Hunter, 1994) was found to contain MTS and thus may be responsible for cyclin B1/Cdk1 influx into mitochondria. However, like many other mitochondrial proteins, cyclin B1/Cdk1 may be relocated to mitochondria via internal signals within the protein sequence and chaperone proteins (Candas et al., 2013; Chacinska et al., 2009).

The G2/M transition requires significant energetic commitments and therefore a timely boost of mitochondrial bioenergetics. The significance of cyclin B1/Cdk1-medicated critical events for processing G2/M transition and the importance of mitochondrial metabolism in supplying cellular ATP generation have been well appreciated over decades. Here, we reveal a mechanism by which the mitochondria can sense and respond to the increased cellular fuel demand during the phase of G2/M transition with cyclin B1/Cdk1-mediated CI activation and enhanced mitochondrial ATP generation, which provides synchronization between mitochondrial activity and G2/M transition to ensure a sufficient energy supply for cell-cycle progression.

EXPERIMENTAL PROCEDURES

Cyclin B1/Cdk1 In Vitro Kinase Assay with 2D Gels

Cyclin B1/Cdk1 kinase assay was performed with established methods (Pan and Hurwitz, 1993). In the presence of phosphatase and protease inhibitors, 1 mg of mitochondrial protein was incubated with 800 units of cyclin B1-Cdk1 in 1,200 μl of 1× kinase assay reaction buffer (50 mM Tris-HCl, 10 mM $MgCl_2$, 1 mM EGTA, 2 mM DTT, 0.01% Brij 35, pH 7.5) supplemented with 100 μM of ATP and 100 μCi/μmol of [γ-^{32}P] ATP at 30°C for 2 hr (Atherton-Fessler et al., 1993). Analysis by 2D SDS-PAGE was performed after 2 hr of reaction. The protocol of cyclin B1/Cdk1 in vitro kinase assay with mitochondria-localized immunocaptured cyclin B1/Cdk1 is presented in the Supplemental Information.

2D Fluorescence Gel Electrophoresis

Mitochondrial protein (1 mg) was used for cyclin B1/Cdk1 kinase assay and then precipitated using 20% TCA before labeling with 400 pmol of Cy2 (GE Healthcare), followed by electrophoresis and staining with Pro-Q Diamond solution (Molecular Probes) and Cy Dye and imaging by Typhoon 9410 laser scanner (Amersham). For 2D-DIGE analysis with [γ-^{32}P] ATP-incorporated phosphorylation, the gel was exposed to phosphoscreen for at least 12 hr and the image was acquired using the Phosphostorage mode.

CI Activity Assay

CI activity was determined by measuring rotenone-sensitive NADH:cytochrome c reductase (NCCR) activity (Martinvalet et al., 2008). The assay was performed with 5 μg of mitochondrial protein in 100 μl of potassium phosphate buffer at 30°C. The oxidation rate of NADH was determined using Spectra Max M^{2e} at the wavelength of 340 nm for 3 min. The assay was also performed in the presence of 5 μM of rotenone to determine the rotenone-insensitive CI activity. For CI rescuing experiments, cells were transfected with CI subunit-specific siRNAs (10–30 nM) and then transfected with the wild-type or mutant CI subunit. CI activity was calculated by subtracting the rotenone-insensitive activity from the total activity of NADH-mediated oxidation rate and was presented as optical density (OD) value.

Oxygen Consumption

Oxygen consumption was determined following reported methods with a Clark-type oxygen electrode (Digital Model 20; Rank Brothers) interfaced with Pico software (PicoLog Recorder and Technology, Interworld Electronics). Ten million cells were suspended in 200 μl of respiration solution (20 mm HEPES, pH 7.1, 250 mm sucrose, 10 mm $MgCl_2$, 2 mm phosphate) and plasma membrane was permeabilized by digitonin (25 μg/ml). Respiration was initiated with the addition of CI substrate glutamate/malate at final concentration of 12.5 mM.

ATP Assay

Cellular ATP content was determined using a luciferase-based ATP assay kit (Molecular Probes). Cells were rinsed twice with cold PBS, 40 μl of cold 0.5% (W/V) trichloroacetic acid (TCA) were added and incubated on ice with shaking for 20 min. Cells were supplemented with 140 μl of 250 mM Tris-Acetate (pH 7.75) per sample, and 10 μl of this cell suspension was mixed with 90 μl of ATP Assay Solution. ATP levels were determined using a Turner TD20/20 Luminometer (Promega).

Detection of Mitochondrial Superoxide

Cells (7 × 10^3) were seeded in 96-well plates and grown for 24 hr before experiments. After treatments, cells were incubated with 5 μM of MitoSOX (Molecular Probes) at 37°C for 10 min, washed 3× with PBS (pH 7.4), and resuspended in 100 μl of PBS. Mitochondrial superoxide was measured at excitation/emission wavelengths of 510/580 nm using Spectra Max M^{2e} plate reader (Molecular Devices).

Statistical Analysis

Data are presented as mean ± SD. Student's t test was used to evaluate two group comparisons and a value of $p < 0.05$ was considered significant.

SUPPLEMENTAL INFORMATION

Supplemental Information includes Supplemental Experimental Procedures, six figures, four tables, and two movies and can be found with this article online at http://dx.doi.org/10.1016/j.devcel.2014.03.012.

AUTHOR CONTRIBUTIONS

Z.W. and M.F. did most of the experiments, including gene transfection, cell synchronization, proteomic analysis, mitochondrial purification, and cell-cycle analysis. T.-Q.Z. and S.W.-H. performed and analyzed the data of mitochondrial relocation of cyclin B1 and CDK1. K.M.A., D.N., and N.D. were involved in mitochondrial purification, western blot, and IP analysis of mitochondrial cyclin B1 and CDK1. D.C. and L.Q. measured mitochondrial cyclin B1 and CDK1 and ATP generation. B.A.C., A.E., and F.H. performed and analyzed the proteomic data. Z.W., M.F., and J.J.L. designed the experiments. Z.W., M.F., D.C., M.C., T.F., L.S.W., and J.J.L. were involved in data discussion and manuscript preparation.

Figure 6. Mitochondrial Cdk1 Is Required for G2/M-Associated Mitochondrial Respiration

(A) Mitochondrial ATP production was measured in the cells treated with 10 μM of RO-3306 or with the solvent control, DMSO, at 2 hr, 6 hr, and 20 hr post-treatment. Data are expressed as percentage over DMSO-treated cells.

(B and C) $\Delta\Psi$m (B) and mitochondrial superoxide (C) production were measured in MCF-10A cells 20 hr after treatment with 10 μM RO-3306 or DMSO.

(D–G) Mitochondrial oxygen consumption, ATP generation, $\Delta\Psi$m, and $O_2\bullet^-$ levels were measured in cells at 48 hr after transfection with the indicated plasmids.

(H–K) Mitochondrial oxygen consumption, ATP generation, $\Delta\Psi$m, and $O_2\bullet^-$ levels were measured in cells with empty vector (pERFP-N1-MTS) or Cdk1-dn mutant (pERFP-N1-MTS-Cdk1-dn) at indicated times after release from G0/G1 synchronization (A–K: mean ± SD; n = 3; *$p < 0.05$; **$p < 0.01$).

See also Figures S4 and S5.

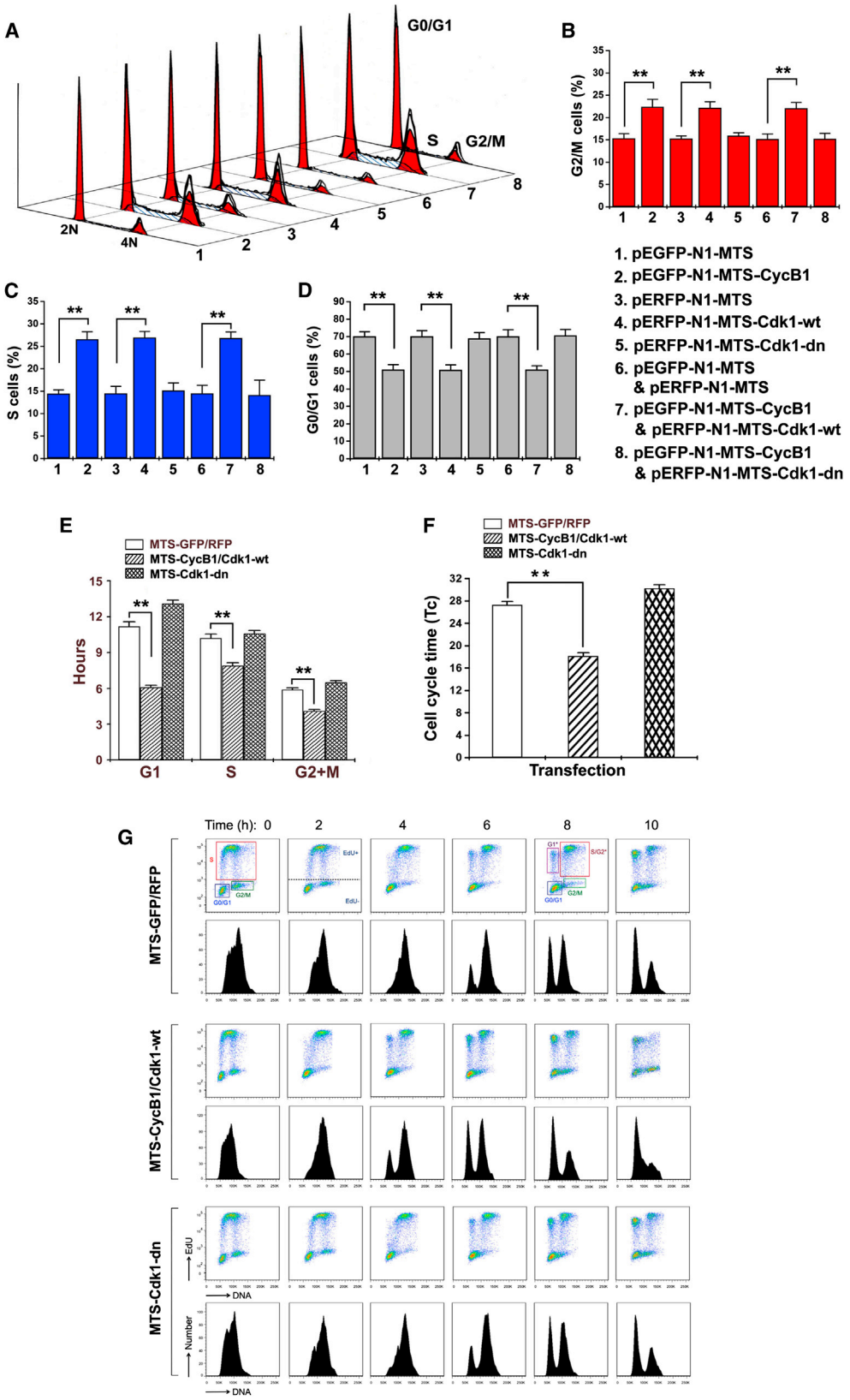

(legend on next page)

ACKNOWLEDGMENTS

We thank Grete Adamson at Electron Microscopy Laboratory, University of California Davis School of Medicine, for technical assistance in mitochondrial analysis and Haiying Hang at Institute of Biophysics, Chinese Academy of Sciences, for analysis of cell-cycle data. This work was supported by NIH grants CA133402 and CA152313 and Department of Energy Office of Science DE-SC0001271 (to J.L.) and the NIH Intramural Research Program of NIDDK (to L.S.W. and T.F.).

Received: March 1, 2012
Revised: October 30, 2013
Accepted: March 18, 2014
Published: April 17, 2014

REFERENCES

Allan, L.A., and Clarke, P.R. (2007). Phosphorylation of caspase-9 by CDK1/cyclin B1 protects mitotic cells against apoptosis. Mol. Cell *26*, 301–310.

Antonyuk, S.V., Han, C., Eady, R.R., and Hasnain, S.S. (2013). Structures of protein-protein complexes involved in electron transfer. Nature *496*, 123–126.

Atherton-Fessler, S., Parker, L.L., Geahlen, R.L., and Piwnica-Worms, H. (1993). Mechanisms of p34cdc2 regulation. Mol. Cell. Biol. *13*, 1675–1685.

Bao, Y., Mukai, K., Hishiki, T., Kubo, A., Ohmura, M., Sugiura, Y., Matsuura, T., Nagahata, Y., Hayakawa, N., Yamamoto, T., et al. (2013). Energy management by enhanced glycolysis in G1-phase in human colon cancer cells in vitro and in vivo. Mol. Cancer Res. *11*, 973–985.

Barnes, E.A., Kong, M., Ollendorff, V., and Donoghue, D.J. (2001). Patched1 interacts with cyclin B1 to regulate cell cycle progression. EMBO J. *20*, 2214–2223.

Baumann, K. (2012). Cell cycle: Order in the pericentriolar material. Nat. Rev. Mol. Cell Biol. *13*, 749.

Candas, D., Fan, M., Nantajit, D., Vaughan, A.T., Murley, J.S., Woloschak, G.E., Grdina, D.J., and Li, J.J. (2013). CyclinB1/Cdk1 phosphorylates mitochondrial antioxidant MnSOD in cell adaptive response to radiation stress. J. Mol. Cell Biol. *5*, 166–175.

Chacinska, A., Koehler, C.M., Milenkovic, D., Lithgow, T., and Pfanner, N. (2009). Importing mitochondrial proteins: machineries and mechanisms. Cell *138*, 628–644.

Claros, M.G., and Vincens, P. (1996). Computational method to predict mitochondrially imported proteins and their targeting sequences. Eur. J. Biochem. *241*, 779–786.

Clute, P., and Pines, J. (1999). Temporal and spatial control of cyclin B1 destruction in metaphase. Nat. Cell Biol. *1*, 82–87.

Davis, P.K., Ho, A., and Dowdy, S.F. (2001). Biological methods for cell-cycle synchronization of mammalian cells. Biotechniques *30*, 1322–1326, 1328, 1330–1321.

Dephoure, N., Zhou, C., Villén, J., Beausoleil, S.A., Bakalarski, C.E., Elledge, S.J., and Gygi, S.P. (2008). A quantitative atlas of mitotic phosphorylation. Proc. Natl. Acad. Sci. USA *105*, 10762–10767.

Draetta, G., and Beach, D. (1988). Activation of cdc2 protein kinase during mitosis in human cells: cell cycle-dependent phosphorylation and subunit rearrangement. Cell *54*, 17–26.

Furukawa, Y., Iwase, S., Kikuchi, J., Terui, Y., Nakamura, M., Yamada, H., Kano, Y., and Matsuda, M. (2000). Phosphorylation of Bcl-2 protein by CDC2 kinase during G2/M phases and its role in cell cycle regulation. J. Biol. Chem. *275*, 21661–21667.

Garedew, A., Andreassi, C., and Moncada, S. (2012). Mitochondrial dynamics, biogenesis, and function are coordinated with the cell cycle by APC/C CDH1. Cell Metab. *15*, 466–479.

Gavet, O., and Pines, J. (2010). Activation of cyclin B1-Cdk1 synchronizes events in the nucleus and the cytoplasm at mitosis. J. Cell Biol. *189*, 247–259.

Harley, M.E., Allan, L.A., Sanderson, H.S., and Clarke, P.R. (2010). Phosphorylation of Mcl-1 by CDK1-cyclin B1 initiates its Cdc20-dependent destruction during mitotic arrest. EMBO J. *29*, 2407–2420.

Hartwell, L.H., and Weinert, T.A. (1989). Checkpoints: controls that ensure the order of cell cycle events. Science *246*, 629–634.

Hunt, T. (1989). Embryology. Under arrest in the cell cycle. Nature *342*, 483–484.

Janssen, R.J., Nijtmans, L.G., van den Heuvel, L.P., and Smeitink, J.A. (2006). Mitochondrial complex I: structure, function and pathology. J. Inherit. Metab. Dis. *29*, 499–515.

Kennady, P.K., Ormerod, M.G., Singh, S., and Pande, G. (2004). Variation of mitochondrial size during the cell cycle: A multiparameter flow cytometric and microscopic study. Cytometry A *62*, 97–108.

Konishi, Y., Lehtinen, M., Donovan, N., and Bonni, A. (2002). Cdc2 phosphorylation of BAD links the cell cycle to the cell death machinery. Mol. Cell *9*, 1005–1016.

Lenormand, J.L., Dellinger, R.W., Knudsen, K.E., Subramani, S., and Donoghue, D.J. (1999). Speedy: a novel cell cycle regulator of the G2/M transition. EMBO J. *18*, 1869–1877.

Martinvalet, D., Dykxhoorn, D.M., Ferrini, R., and Lieberman, J. (2008). Granzyme A cleaves a mitochondrial complex I protein to initiate caspase-independent cell death. Cell *133*, 681–692.

Mitra, K., Wunder, C., Roysam, B., Lin, G., and Lippincott-Schwartz, J. (2009). A hyperfused mitochondrial state achieved at G1-S regulates cyclin E buildup and entry into S phase. Proc. Natl. Acad. Sci. USA *106*, 11960–11965.

Nakada, D., Saunders, T.L., and Morrison, S.J. (2010). Lkb1 regulates cell cycle and energy metabolism in haematopoietic stem cells. Nature *468*, 653–658.

Nantajit, D., Fan, M., Duru, N., Wen, Y., Reed, J.C., and Li, J.J. (2010). Cyclin B1/Cdk1 phosphorylation of mitochondrial p53 induces anti-apoptotic response. PLoS ONE *5*, e12341.

Neupert, W., and Herrmann, J.M. (2007). Translocation of proteins into mitochondria. Annu. Rev. Biochem. *76*, 723–749.

Nurse, P.M. (1990). Universal control mechanism regulating onset of M-phase. Nature *344*, 503–508.

O'Connor, D.S., Wall, N.R., Porter, A.C., and Altieri, D.C. (2002). A p34(cdc2) survival checkpoint in cancer. Cancer Cell *2*, 43–54.

Owusu-Ansah, E., Yavari, A., Mandal, S., and Banerjee, U. (2008). Distinct mitochondrial retrograde signals control the G1-S cell cycle checkpoint. Nat. Genet. *40*, 356–361.

Figure 7. Mitochondrial Cdk1 Enhances G2/M Transition and Overall Cycle Progression

(A–D) Cell population kinetics in cells at 48 hr after transfection with indicated mitochondria-targeted cyclin B1, Cdk1, cyclin B1/Cdk1, and control vectors; a representative plot (A), and percentage in G2/M (B), S (C), and G0/G1 (D) phases are presented (mean ± SD; n = 3; $^{**}p < 0.01$).

(E and F) Cell-cycle progression including the duration of G1, S, G2/M phases (E), and cell-cycle time (Tc; F) were determined based on the flow cytometry analysis of the DNA content (mean ± SD; n = 3; $^{*}p < 0.05$; $^{**}p < 0.01$). See also Figure S6 and Table S4.

(G) Cell-cycle analysis with EdU pulse-chase labeling. Cells were pulsed with EdU for 30 min followed by 24 hr transfection with indicated constructs on the left. The EdU-positive population was followed over time as it progressed through cell-cycle phases. Scatter plot histograms of EdU-labeled cells were stained for DNA content (x axis) and EdU (y axis). The lower figures in each panel show the mean fluorescence intensity of the EdU-labeled nuclei. The time points were indicated in hr after the EdU pulse. For all time points, gates displaying the following populations were drawn: G0/G1, S, and G2/M. For 6, 8, and 10 hr time points, EdU-labeled G1*, S/G2*, and G2/M* populations are shown.

Pagliarini, D.J., and Dixon, J.E. (2006). Mitochondrial modulation: reversible phosphorylation takes center stage? Trends Biochem. Sci. *31*, 26–34.

Pan, Z.Q., and Hurwitz, J. (1993). Reconstitution of cyclin-dependent cdc2 and cdk2 kinase activities in vitro. J. Biol. Chem. *268*, 20433–20442.

Pathan, N., Aime-Sempe, C., Kitada, S., Basu, A., Haldar, S., and Reed, J.C. (2001). Microtubule-targeting drugs induce bcl-2 phosphorylation and association with Pin1. Neoplasia *3*, 550–559.

Pines, J., and Hunter, T. (1994). The differential localization of human cyclins A and B is due to a cytoplasmic retention signal in cyclin B. EMBO J. *13*, 3772–3781.

Roessler, M.M., King, M.S., Robinson, A.J., Armstrong, F.A., Harmer, J., and Hirst, J. (2010). Direct assignment of EPR spectra to structurally defined iron-sulfur clusters in complex I by double electron-electron resonance. Proc. Natl. Acad. Sci. USA *107*, 1930–1935.

Sakamaki, T., Casimiro, M.C., Ju, X., Quong, A.A., Katiyar, S., Liu, M., Jiao, X., Li, A., Zhang, X., Lu, Y., et al. (2006). Cyclin D1 determines mitochondrial function in vivo. Mol. Cell. Biol. *26*, 5449–5469.

Schieke, S.M., McCoy, J.P., Jr., and Finkel, T. (2008). Coordination of mitochondrial bioenergetics with G1 phase cell cycle progression. Cell Cycle *7*, 1782–1787.

Schmitt, E., Beauchemin, M., and Bertrand, R. (2007). Nuclear colocalization and interaction between bcl-xL and cdk1(cdc2) during G2/M cell-cycle checkpoint. Oncogene *26*, 5851–5865.

Schulz, T.J., Thierbach, R., Voigt, A., Drewes, G., Mietzner, B., Steinberg, P., Pfeiffer, A.F., and Ristow, M. (2006). Induction of oxidative metabolism by mitochondrial frataxin inhibits cancer growth: Otto Warburg revisited. J. Biol. Chem. *281*, 977–981.

Sweet, S., and Singh, G. (1995). Accumulation of human promyelocytic leukemic (HL-60) cells at two energetic cell cycle checkpoints. Cancer Res. *55*, 5164–5167.

Sweet, S., and Singh, G. (1999). Changes in mitochondrial mass, membrane potential, and cellular adenosine triphosphate content during the cell cycle of human leukemic (HL-60) cells. J. Cell. Physiol. *180*, 91–96.

Taguchi, N., Ishihara, N., Jofuku, A., Oka, T., and Mihara, K. (2007). Mitotic phosphorylation of dynamin-related GTPase Drp1 participates in mitochondrial fission. J. Biol. Chem. *282*, 11521–11529.

Takizawa, C.G., and Morgan, D.O. (2000). Control of mitosis by changes in the subcellular location of cyclin-B1-Cdk1 and Cdc25C. Curr. Opin. Cell Biol. *12*, 658–665.

Terry, N.H.A., and White, R.A. (2006). Flow cytometry after bromodeoxyuridine labeling to measure S and G2+M phase durations plus doubling times in vitro and in vivo. Nat. Protoc. *1*, 859–869.

Truscott, K.N., Brandner, K., and Pfanner, N. (2003). Mechanisms of protein import into mitochondria. Curr. Biol. *13*, R326–R337.

van den Heuvel, S., and Harlow, E. (1993). Distinct roles for cyclin-dependent kinases in cell cycle control. Science *262*, 2050–2054.